Sustainable Structures
ISSN: 2789-3111 (Print); ISSN: 2789-312X (Online)
http://www.sustain-dpl.com/journal/sust
DOI: 10.54113/j.sust.2025.000087

ORIGINAL ARTICLE

Impact of accurate reinforcement steel assessment on structure longevity and progressive collapse resistance

Omer Ghunaim[a], Said Elkholy[b], Osama H. Galal[c], Bilal El-Ariss[a,*]

[a]Department of Civil and Environmental Engineering and Emirates Center for Mobility Research, United Arab Emirates University, P.O. Box 15551, Al Ain, United Arab Emirates
[b]Department of Civil Engineering, Fayoum University, P.O. Box 63514, Fayoum, Egypt
[c]Department of Engineering Mathematics and Physics, Fayoum University, P.O. Box 63514, Fayoum, Egypt
[*]Corresponding Author: Bilal El-Ariss. Email: bilal.elariss@uaeu.ac.ae

Abstract: Current standards for reinforcement steel may not accurately reflect the actual properties of steel used in construction, leading to potentially underestimating the resistance and longevity of structures. The study discusses the discrepancy between minimum permissible steel properties required by current standards such as ASTM A615/A615M, BS 4449:2005, and ES 262-2/2015 and actual properties of steel frequently used in construction and its impact on the sustainability and progressive collapse resistance of reinforced concrete structures. This discrepancy may lead to false sense of how sustainable and reliable structures are against progressive collapse. The study employs two-dimensional fiber element models to simulate the behavior of structures under progressive collapse. The study quantifies the difference in mechanical properties between actual steel used in construction and the standards it should meet. Correlation relationships are developed to forecast the structure progressive collapse behavior and ductility using the structure known material mechanical properties. Tests of hypothesis and confidence intervals are employed to draw conclusions and demonstrate the impact of underestimating steel properties on the structure longevity and resistance to progressive collapse. This study addresses a crucial aspect of structure design by highlighting the importance of using accurately steel properties to ensure safety and longevity of structures.

Keywords: Progressive collapse, reinforcement steel, catenary action, reliability index, confidence intervals, test of hypothesis, finite element modeling

1 Introduction

The progressive collapse phenomenon occurs as a result of structural damage in a localized area, leading to the collapse of adjacent elements, which then triggers further collapse [1]. This phenomenon has been observed in several major events like the 1968 Ronan Point building (UK), 1995 Murrah Federal Building (US), 2001 World Trade Center (US), and 1986 New World Hotel (Singapore) [2], [3]. These events have raised concerns related to the adopted building guidelines and practices. Several design standards and guidelines have developed provisions and recommendations for designing against progressive collapse [1], [4], [5], [6]. For example, guidelines by GSA, General Services Administration [1], and DOD, U.S. Department of Defense (DOD) [7], suggest that the progressive collapse resistance can be estimated based on the structural resistance against several vertical element removal scenarios

Received: 30 October 2024; Received in revised form: 4 September 2025; Accepted: 29 August 2025

through APM, Alternate Path Method [8] [9]. Other design standards use the term "robustness" to describe a structural attribute that denotes the resistance to local failure and the capability of a structure to withstand damage without major failure [10]. The Eurocode 1 defines it as the structure's capacity to survive calamities such as fire, explosions, impact, and human error without causing excessive damage [4].

The severe consequences of the structure progressive collapse have intensified various experimental and numerical investigations on the structure progressive collapse resistance. El-Ariss et al. [11] invented a mitigating scheme comprising steel reinforcement/rebar embedded within the thickness of reinforced concrete floor and placed around a potentially failed column to upgrade progressive collapse resistance of framed structures. Weng et al. [12] presented criteria to assess flexural, shear, and axial damages during numerical analysis of reinforced roncrete (RC) frame exposed to progressive failure using 2D fiber element model. Abedini and Mutalib [13] presented a set of variations in a damage index for reinforced concrete structures under different blast load scenarios, offering an overview of damage criteria and examining the modes of failure when subjected to explosive loads. Sangiorgio et al. [14] suggested a unique damage index designed particularly for blast loading on RC structures, which provides important insights into damage mechanisms under high loading circumstances. Abedini and Zhang [15] numerically evaluated the blast load-behavior of un-strengthened and FRP-strengthened RC columns subjected. Scalvenz et al. [16] numerically investigated the effect of CFRP strengthening on the robustness of low-rise RC frame buildings designed to resist gravity loads in accordance with Eurocode standards. Kumar et al. [17] presented a comprehensive review of recent research on the resistance of RC frames to progressive collapse, including multiple damage assessments and evaluation techniques. Very few studies can be found in the literature with an aim at employing a probability-based analysis when examining progressive collapse of structures. For example, Ellingwood and Galambos [18] presented a thorough framework for the probability-based design of RC buildings, including methods for incorporating uncertainty into structural analysis and design. Le and Xue [19] developed a stochastic numerical model for probabilistic analysis to examine the collapse behavior of 2D reinforced concrete frames in response to specified local structural damage. Li et al. [20] evaluated the progressive collapse resistance of RC structures by proposing a probabilistic index by performing an APM analysis considering all possible initial local failure schemes outlined in current code regulations. Ibrahim et al. [9] investigated the structural resilience against progressive collapse in cases of column or shear wall removal at various tiers using deterministic analysis. Moreover, several reliability-based studies have been carried out to assess the resistance of gradual collapse of RC frames [21], [22], [23]. Zhou et al. [24] presented a reliability-based study of gradual collapse behavior of fully assembled pre-cast structural frames.

The aforementioned studies emphasized on the behavior of the structural system whether being an ordinary, special or retrofitted RC frame evaluating its strength, resistance and/or robustness. However, material properties portray a significant contribution to the behavior of the structure under progressive collapse which attracted scholars to further research this topic. Previous studies [25], [26], [27], [28] indicated that randomness in material’s mechanical properties and geometric sizes can result in variations in failure resistance of the structure. Other investigations have addressed impact of corrosion in steel on the gradual collapse resistance of buildings [29], [30], [31], [32]. Feng et al. [33] proposed a probabilistic approach for assessing the redundancy of both corroded and uncorroded structures during disproportionate collapse, utilizing time-dependent reliability indicators derived from the probability density evolution method (PDEM). Elsayed et al. experimentally evaluated the impact of reinforcement debonding on the gradual failure resistance of framed buildings designed as per provisions of the Egyptian seismic design code. Jagatheswari et al. [35] studied the performance of multiple bare RC buildings of various stories and different steel grades subjected to column elimination scenarios with nonlinear static conditions. Alrubaidi et al. [36] employed numerical investigations on mitigating gradual failure of steel beam–column joint by means of steel plates of different grades (A36 and A572). It was concluded that the average enhancement in ultimate load due to varying the plate thickness was around 22% and 8% for grades A36 and A572, respectively, while the A572 steel plates amplified the ultimate load by 30%. Shaijal et al. [28] assessed the Robustness index as an indicator for resistance against collapse of the structure after considering uncertainties (aleatory or epistemic) to calculate a adjustment parameter for the capacity reduction factor, R, which could subsequently be incorporated in

design code guidelines to address the implications of material uncertainty in construction.

Standards such as American Society for Testing and Materials Standard Specification for Deformed and Plain Carbon-Steel Bars for Concrete Reinforcement (ASTM A615/A615M) [37], British Standards Institution Criteria of Steel for the Reinforcement of Concrete (BS 4449:2005) [38], and Egyptian Standard for Steel Bars (ES 262-2/2015) [39] obligate engineers to test steel bars to ensure that the bar steel material properties comply with the minimum permissible properties either chemically, physically or mechanically. Construction materials, mainly reinforcement steel in this study, used in the design of structures show higher mechanical properties than the adopted standard material minimum permissible properties. This discrepancy between the minimum permissible and actual property values of the steel bars can lead to underestimating the structure actual disproportionate collapse resistance. This disparity is, hence, thought to be the cause why some structures remain standing still despite of some of their column visible collapses, as shown in **Fig. 1.** Although a major load carrying component was damaged, progressive collapse did not materialize.

Fig. 1. Building remains standing after column loss [40]

Based on the above-mentioned review, no studies could be found in the literature that address the impact of the discrepancy between the minimum permissible steel properties required by current standards and the actual properties of steel frequently used in construction on the structures progressive collapse resistance and longevity. In the absence of such studies, this paper aims to fill in this gap. The novelty of this study is the assessment of how reliable a steel grade/standard is in the structure resistance to gradual collapse. Two-dimensional fiber element models were employed and several key statistics of several steel samples following different standards were used to show how mechanically different the actual steel used in construction is compared with the adopted standard and to demonstrate that steel with higher mechanical properties improve the structure longevity and resistance. In addition, correlation relationships were constructed to predict some structural outputs related to the progressive collapse behavior. Finally, statistical methods such as tests of hypothesis and confidence intervals were used to draw conclusions.

This study presents a novel examination of the discrepancies between the actual mechanical properties of reinforcement steel utilized in construction and the minimum acceptable properties specified in design standards. It further explores the implications of these discrepancies on the longevity and resistance of RC buildings to disproportionate failure. Using two-dimensional numerical models and statistical tools, the study quantifies these differences, establishes predictive correlations for structural behavior, and underscores the critical importance of accurately estimating material properties to augment the longevity and resistance of structures to gradual failure.

2 Steel Grades and Standards

The relation between concrete and steel reinforcement is crucial to the performance of reinforced concrete structures. This interaction is characterized by several important factors such as bond characteristics between concrete and steel, load transfer mechanisms, and material property influence on the overall behavior of the structure. If a localized failure occurs, such as loss of column, interaction between the concrete and steel plays a vital role in redistributing the loads throughout the structure. The steel capacity to support and re-distribute load when concrete is compromised is essential for averting progressive collapse. Steel is a combination of iron and carbon reinforced with other alloying elements.

It has different chemical compositions and production procedures, resulting in a wide range of steel grades. These grades exhibit a variety of characteristics and are employed for different purposes. To control these variations, engineers and manufacturers rely on steel standards, which serve as critical frameworks for categorizing, analyzing, and distinguishing the material, chemical, mechanical, and metallurgical properties of various steel grades. These criteria are critical in the manufacturing of reinforcement steel bars [41].

Standards are primarily used to set the minimum acceptable mechanical properties, chemical compositions, testing procedures, and specific physical features. As a result, a steel specimen created in accordance with a certain standard must meet the defined constraints to be considered suitable for construction. Thus, steel used in the construction industry often requires mechanical properties that meet or exceed the values specified in the standards.

Steel standards could be internationally used or even developed locally. Prominent examples of widely employed global standards include ASTM A615/A615M [37] and BS 4449:2005 [38], while standards such as ES 262-2/2015 [39] serves as a domestically formulated steel standard adopted within the Arab Republic of Egypt. These standards include a range of grades with diverse chemical, physical, and mechanical properties. In this study, particular focus is directed towards ASTM A615/A615M Grade 60, BS 4449:2005 B500B, and ES DWR B500B. **Tables 1** and **2** appended herein summarize the minimum mechanical properties and chemical compositions corresponding to each grade, respectively.

Table 1. Minimum Mechanical Properties of Steel Grades

Steel grade	Minimum Yield Strength*	Minimum Tensile Strength*	Minimum Elongation %
ASTM A615/A615M Gr60 [37]	420	620	7%
BS 4449:2005 B500B [38]	500	540	5%
ES DWR B500B [39]	500	650	8%

*Values are in MPa

Table 2. Chemical Composition of Steel Grades

Steel grade	Chemical Composition (maximum % by mass)							
	C	S	P	N	Cu	Mn	Si	CEV*
ASTM A615/A615M Gr60 [37]	-	-	0.066	-	-	-		-
BS 4449:2005 B500B [38]	0.24	0.055	0.055	0.014	0.85	-	-	0.52
ES DWR B500B [39]	0.32	0.04	0.04	0.012	-	1.8	0.55	0.61

* CEV stands for “Carbon Equivalent Value”

3 Fiber Element Modeling

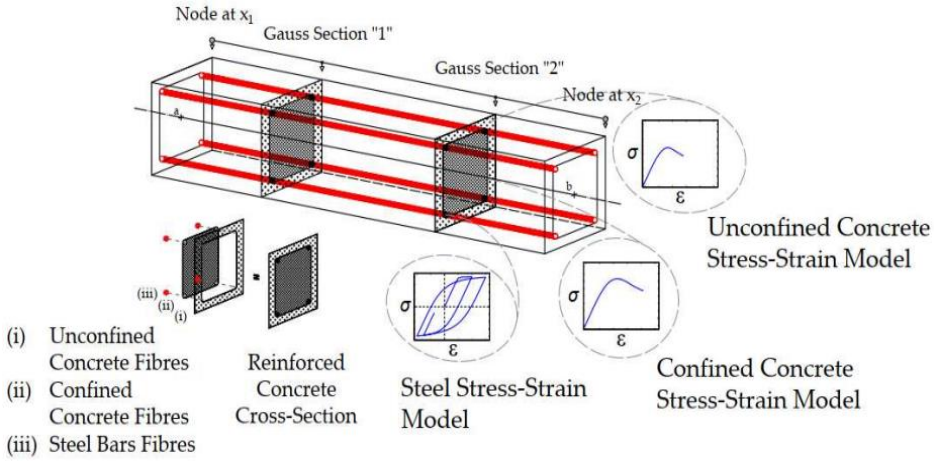

Fig. 2. Discretization of a typical reinforced concrete cross-section [43]

In this study, the finite element program SeismoStruct [42] was employed in this study fiber-element-based numerical model to account for the structure geometrical nonlinearity and material

inelasticity when simulating the structure gradual collapse behavior due to column exclusion. The member cross-section is modeled as distinct fibers characterizing steel and concrete materials separately, as displayed in **Fig. 2.** These fibers are assigned corresponding concrete and steel material stress-strain models. The stress-strain states of the fibers at any cross-section are then computed by integration of stress-strain states of the individual fibers, which are typically numbered 100 to 150 and partitioned into the section. In addition, the distribution of plasticity throughout the element is numerically derived by integrating equations of equilibrium using nonlinear cubic formulation with two Gauss points. **Fig. 2.** illustrates the detachment of typical RC cross section using the aforementioned technique.

To forecast the disproportionate collapse performance of framed structure, displacement-controlled push-down was performed at the removed column location. As the push-down was gradually increased, the strains and stresses in the different fibers were computed and compared against a predefined set of material damage criteria that defined the damage types and traced their sequence. The sum of the reactions generated in all the columns of the frame as a result of the push-down displacement represented the load applied at the failed column location. A typical load-vertical displacement (deflection) curve at the location of failed column is depicted in **Fig. 3.** with key points identified on the curve and energy types labelled beneath the curve.

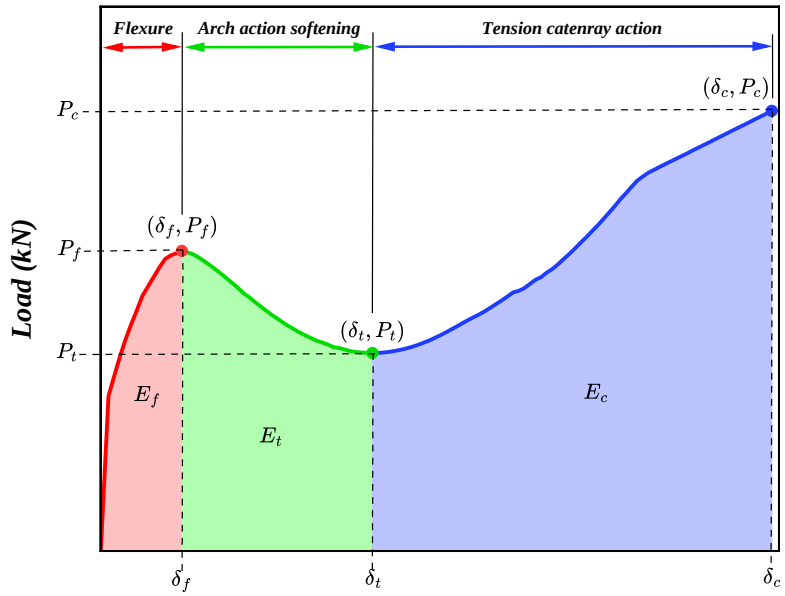

P_f, δ_f = First peak load and its corresponding deflection

P_t, δ_t = Low peak load at the bottom of the softening curve and its corresponding deflection

P_c, δ_c = Load at max. catenary action capacity and its corresponding deflection

E_f = Flexure action energy dissipated

E_t = Arch action softening energy dissipated

E_c = Tension catenary action energy dissipated

Total Energy $(E_{tot}) = E_f + E_t + E_c$

Fig. 3. Major points and areas under the graph for the pushdown curve

4 Numerical Modeling

This study is twofold: numerical modelling and simulations using Seismostruct software and statistical analysis. The statistical analysis is addressed in the sections below.

Seismostruct stands out as a finite element software tool designed exclusively for structural analysis. Its strong capabilities include successfully estimating the significant deformation responses of frames exposed to static or dynamic loading situations while accounting for geometric nonlinearities and material inelasticity [42]. Leveraging these inherent features, the research conducts a thorough

evaluation of the consequences of using various steel grades with differing mechanical properties. The study considered 2D RC frame with no slabs as one of the approaches regularly utilized by many researchers in investigating progressive collapse of structures. Modelling structures as 2D RC frames may not be perfect structure but it can provide fairly acceptable findings and; hence, it has become a viable approach that has been frequently and widely used by researches. Large number of studies that model structures as 2D RC frames in the investigation of disproportionate failure behavior are readily available in the literature. As one example of these studies that have modelled structures as 2D RC frame with no slabs is a study by Le and Xue [19]. The numerical model used in this study was comprehensively verified by the authors in prior published study (experimental evidence is found in reference [43] in the manuscript). In that work, an extensive database was compiled, comprising experimental results from 29 different tests on RC frames and RC sub-assemblages related to progressive collapse scenarios. This database was used for comparison, tuning, and validation of the utilized numerical model. The validated numerical model was also used in previous published work [44], [45], [46], [47], [48] by the authors showing accurate structural responses. Therefore, the validated model was employed for producing the numerical simulations in this study (experimental evidence to support the validation of the model can be found in reference [43]). To investigate and compare the actual performance of reinforcement steel with different specifications, three samples sized 286, 27, and 37 steel specimens were collected from various laboratories complying with the specification standards of BS 4449/05 Gr B500B, ASTM A 615 GR 60, and B500 DWR, which are briefly designated as S1, S2, and S3, respectively. Each specimen was tested for its yield stress, tensile stress, and elongation to be used as input data. This data is then utilized to obtain the structure responses to progressive collapse such as flexure (δ_f, P_f), arch (δ_t, P_t), and catenary (δ_c, P_c) key points as well as the energy consumed for flexure (E_f), arch (E_t), catenary (E_c) and total energy (E_{tot}) as outputs. These outputs for each specimen, as well as the same outputs for each specification Standard value of inputs, were obtained using the Seismostruct software.

4.1 Framed Structure Used in the Study

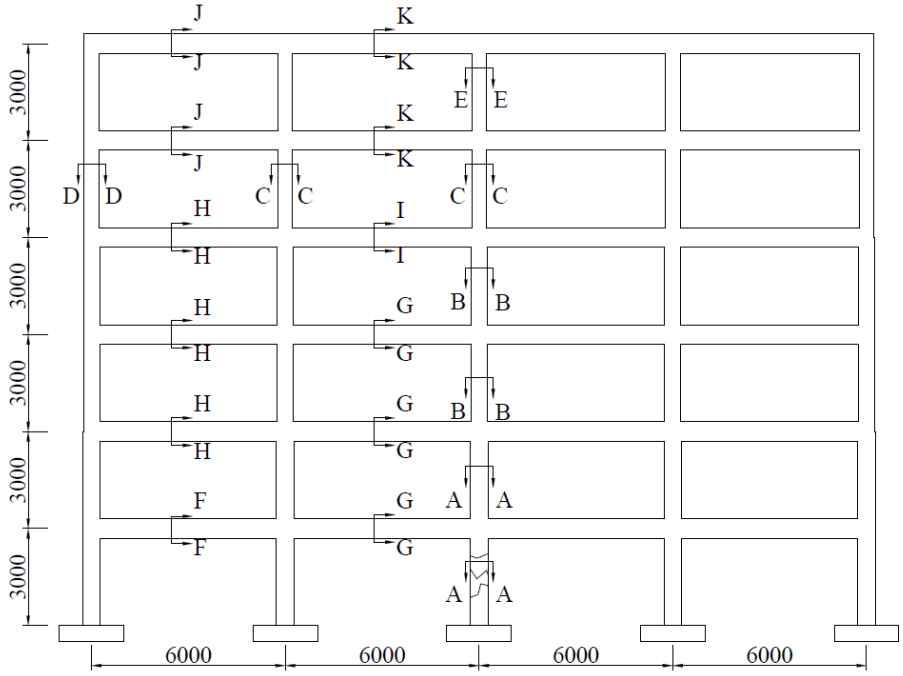

Fig. 4. Design details of the RC test frame specimen (Unit: mm).

Fig. 4. shows a schematic representation of the four-bay six-story RC 2D framed building considered in this study. The 2D frame features a 6-meter center-to-center spacing between columns and a 3-meter story height. The longitudinal reinforcement employed in the considered building beams and columns were deformed bars of diameters ranging from 14 mm to 20 mm. Ties and stirrups of 10

mm diameter were included at spacings of 100 mm and 125 mm for columns and beams, respectively. The frame is symmetrical around the vertical axis that passes through the middle columns. All columns of each floor have the same cross-section, as shown in **Fig. 4.** Detailed reinforcement configurations for both beams and columns are precisely outlined in **Fig. 5.** and **Table 3** for a comprehensive explanation. All sections were modeled as inelastic plastic-hinge force-based frame element "infrmFBPH" which is an option that is suitable for most practical applications [42]. Middle column of ground floor was considered as failed column. It should be noted that the use of 2D fiber element models has been well-documented in the literature verifying their effectiveness in predicting the behavior of RC structures with different loading conditions, including progressive collapse. While 2D fiber element models offer a robust and efficient means of simulating the gradual collapse of buildings, it is essential to recognize their limitations and the potential for overlooking critical out-of-plane effects. For in-depth investigation on the implications of out-of-plane behavior on the overall structural response, 3D analysis could be used to complement the 2D analysis. However, with careful interpretation of the 2D findings, 2D models can provide valuable insights and help in understanding the fundamental mechanisms of failure without the added complexity of 3D models, making it a practical choice for preliminary assessments and simulations or when resources are limited. This efficiency allows for the analysis of larger structures or more complex scenarios within a reasonable timeframe.

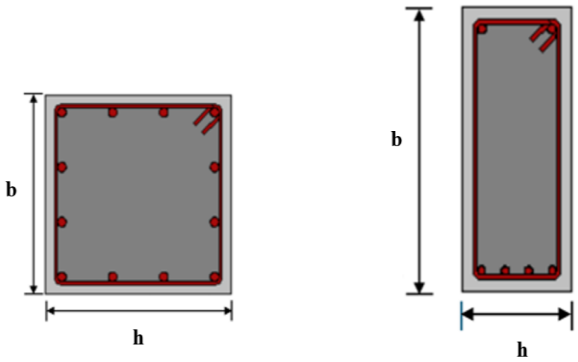

Fig. 5. Beams and Columns cross-sections

Table 3. Section details of beams and columns

Section	Geometry		Main reinforcement			Ties/stirrups	
	h /mm	*b* /mm	Cover /mm	*As*, Top	*As*, Bottom	Size	Spacing /mm
A-A	550	550	50	12#18		#10	100
B-B	500	500	50	12#18		#10	100
C-C	450	450	50	12#16		#10	100
D-D	450	450	50	12#18		#10	100
E-E	450	450	50	12#20		#10	100
F-F	600	250	50	2#20	4#18	#10	125
G-G	600	250	50	3#20	2#18	#10	125
H-H	600	250	50	2#20	4#18	#10	125
I-I	600	250	50	3#20	3#18	#10	125
J-J	600	250	50	4#14	4#18	#10	125
K-K	600	250	50	2#18	2#18	#10	125

4.2 Material Properties of the Framed Structure

The concrete material was modeled using the nonlinear concrete model (con_ma) of Mander et al., which is embedded in the library of Seismostruct [42]. The input material properties needed for this model are the cylinder 100 × 200 mm compressive strength, tensile strength, modulus of elasticity, strain at peak stress, and specific weight. The average 28-day concrete compressive strength for all stories was 35 MPa while the tensile strength was 2.2 MPa (default value). The modulus of elasticity was 27.8 GPa with strain at peak stress of 0.002 (default value). Finally, the specific weight was 24 kN/m^3 (default value). The properties of concrete are constant for all models.

As for the reinforcement, laboratory tests of 376 steel specimens from different manufacturers and universities were obtained. The specimen mechanical properties are presented in **Fig. 6.** to **Fig. 8.** and **Table 4**. The reinforcement was modelled using the Bilinear steel model (stl_bl) which is also found in the library of Seismostruct. This model encompasses both elastic and plastic responses of the reinforcement steel. In the elastic phase, the stress and strain relation is linear. Upon reaching the yield strength of the steel, it transitions into the plastic region, where it demonstrates strain hardening, resulting in an increase in stress with further increase in strain. The material properties needed for this model are the modulus of elasticity, yield strength, strain hardening parameter, fracture/buckling strain and the Specific Weight. The Strain Hardening Parameter is defined using **Eq. (1)** [42] that has been specified by the software library [42]. The modulus of elasticity and specific weight have values of 200 GPa and 78 kN/m^3 respectively for all specimens.

$$\mu = \frac{f_u - f_y}{E\left(\varepsilon_{ult} - \frac{f_y}{E}\right)} \tag{1}$$

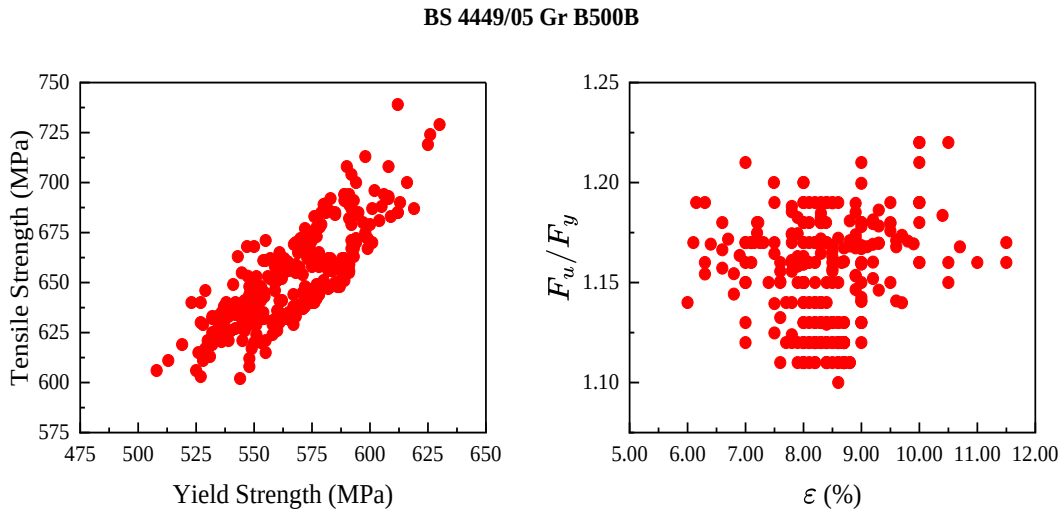

Fig. 6. Mechanical properties of tested specimens (S1)

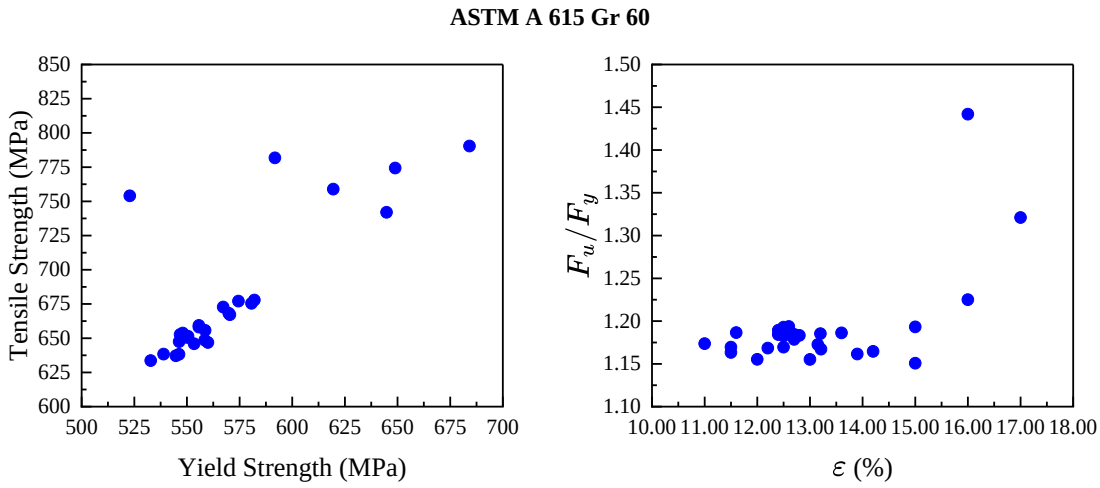

Fig. 7. Mechanical properties of tested specimens (S2)

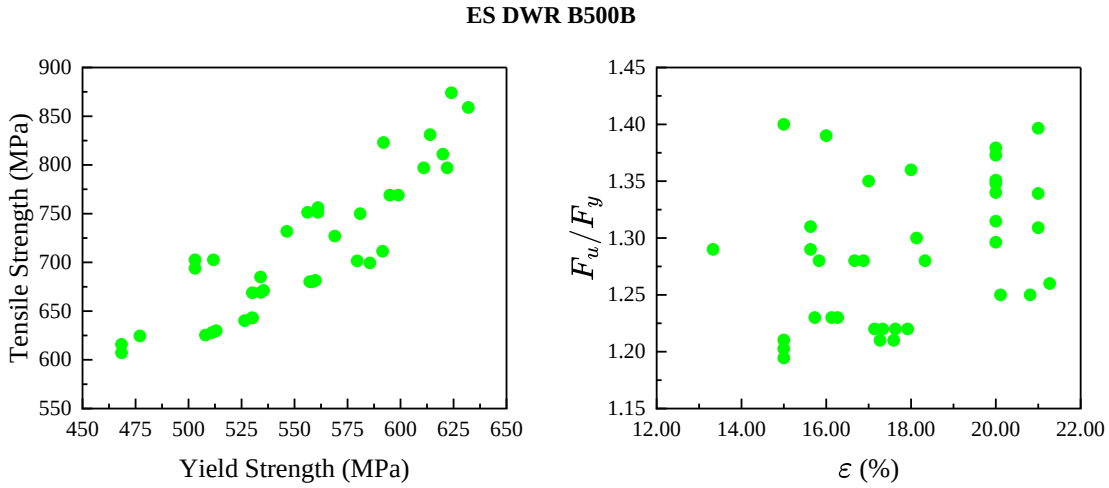

Fig. 8. Mechanical properties of tested specimens (S3)

Table 4. Summary of steel specimens' mechanical properties

Spec	# of specimens	F_y[a]	F_u[a]	Elongation	F_u/F_y
S1	286	508 - 630	602 - 739	6% - 12%	1.10 - 1.22
S2	27	522.9 - 684.2	633.6 - 790.4	11% - 17%	1.15 - 1.44
S3	37	468.39[b] - 632	607.18[b] - 874	13% - 21%	1.19 - 1.40

[a] All values are in MPa.

[b] Some samples have properties lesser than the minimum allowable

5 Results and Discussion

5.1 Numerical Analysis Results

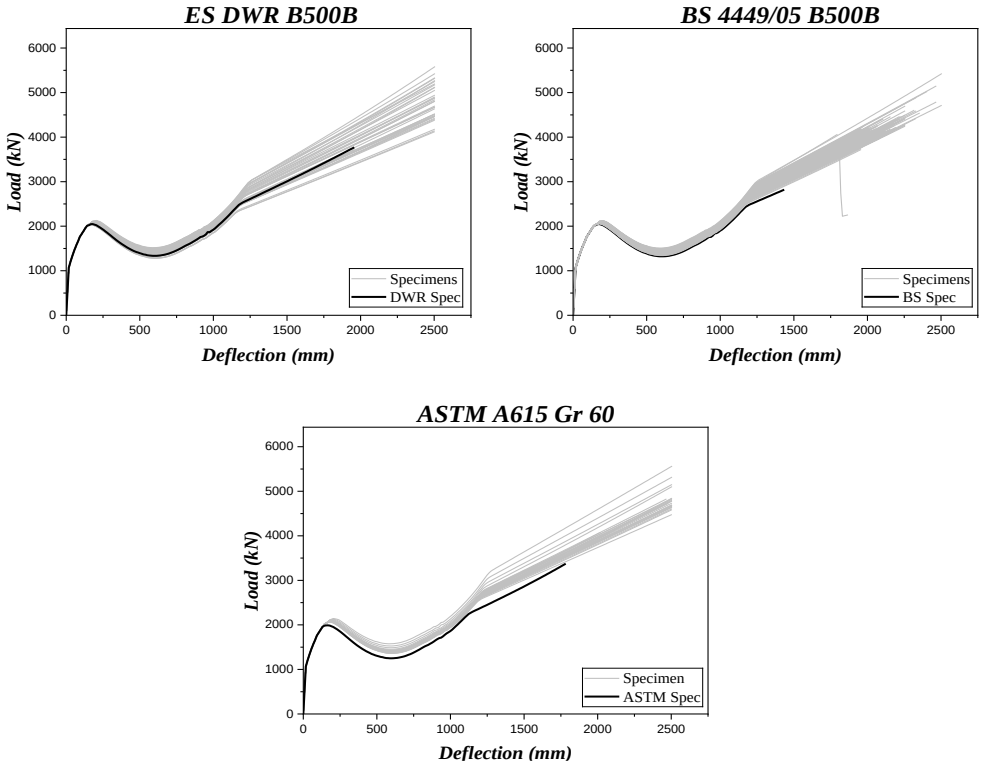

Fig. 9. Load-deflection curves of structures with steel reinforcement used in the specimens and structures with steel reinforcement in compliance with standards.

As discussed in a previous section, a pushdown analysis is performed on a total of 376 modeled 2D RC frames with the geometry and material properties presented in sections 4.1 and 4.2. All models had the same concrete properties as defined in section 4.2 but are different in the steel mechanical properties. **Fig. 9.** shows the load-deflection (deflection is the downward displacement at the excluded column location) curves for structure with steel bar mechanical property values used in the samples and structure with steel bar mechanical values complying with the standards.

The curves in **Fig. 9.** reveal that although all frames for a respective standard had different steel properties, there is a very mild change in the flexural and arch action softening behavior. Moreover, the figure demonstrates that the deflection for the flexural and arch action softening of the progressive collapse was slightly increased while a higher peak load and a larger deflection/ductility at the maximum catenary capacity compared to the respective standard steel properties were evident. **Fig. 9.** demonstrates that the standards potentially undermine the ductility and; therefore, the longevity of the structures. In addition, the slopes of the curves during the catenary action phase exhibit variations, indicating differences in stiffness. The area under each curve, representing the energy absorbed, differs from one sample to another. Although the final (maximum) deflection appears similar across most curves, there are subtle differences. **Table 5.** provides strong evidence supporting this claim, as the standard deviation (*S*) for final (maximum) deflection δ_c is not zero for any of the three specifications, albeit very small, indicating low variance. Further discussion on the final displacement is presented in section 5.2.

5.2 Analysis of Key Statistics and Correlations

The histogram and Probability Density Function (PDF) curves for the samples of the three specifications are shown in **Fig. 10.** to **Fig. 13.**, representing yield stress, tensile stress, elongation, and ratio. Both curves were scaled to unity for easier comparison. The input and output data for each specimen was normalized by dividing it by the corresponding specification value, expressing it as a ratio of the Standards. The histograms show the behavior of the sample, while the PDF approximates the behavior of the entire population, from which the sample was drawn. **Fig. 10.** and **Fig. 11.** indicate that S2 performs better in yield and tensile stress, while **Fig. 12.** and **Fig. 13.** show that S3 and S1 have higher values in elongation and ratio. Additionally, the PDF of the obtained data closely resembles a Gaussian distribution in all four figures.

Furthermore, the MATLAB software was also used to calculate the required key statistics for each specification, consisting of four inputs and eight outputs [49]. These evaluated statistics included the mean $(\bar{x})$, standard deviation (S), minimum (min), maximum (max), range (R), reliability index $(R.I.)$ as well as the upper bound (*U.B.*) and lower bound (*L.B.*) for 99% confidence intervals $(C.I.)$. Moreover, the $R.I.$ for the collected sample and $(1-\alpha)$ confidence interval for the population is given by **Eq. (2)** and **(3)** respectively [50], [51].

$$R.I. = \frac{\bar{x}}{S} \tag{2}$$

$$C.I. = \left(\bar{x} - \frac{S \times t_{\alpha/2,n}}{\sqrt{n}}, \bar{x} + \frac{S \times t_{\alpha/2,n}}{\sqrt{n}} \right) \tag{3}$$

providing that $t_{\alpha/2,n}$ is the value of t-distribution with n-degrees of freedom achieving $P(T \leq t_{\alpha/2,n}) = (1-\alpha/2)$, and n is the sample size. In addition, these evaluated key statistics were tabulated in **Table 5**, while **Table 6** and **Table 7** included the correlation coefficients and their descriptions between the inputs and outputs.

As a result, the analyzed figures and statistics have highlighted several key findings. Regarding the yield stress, S2 provided the best $(\bar{x}/F_y)$, higher (min/F_y) and (max/F_y) with higher upper $(U.B./F_y)$ and lower bounds $(L.B./F_y)$ for *C.I.* valued at 135.83%, 124.50%, 162.90%, 131.03% and 140.64%, respectively. In addition, S1 provided the highest *R.I.*, lowest (S/F_y), and lowest (R/F_y) with values of 24.43, 4.63%, and 24.40%, respectively. In what concerns the tensile stress, S1 has shown the best

statistics in all studied items except (max/F_u), which was higher in S3 with a value of 139.84%. It was observed also that S3 had minimum values of 93.68% and 96.80% for both (min/F_y) and (min/F_u) respectively, which doesn't meet the standards' one. The total readings that violated the standard's minimum value for S3 were 4 specimens out of 37, i.e. 10.81%. Investigating the elongation statistics, S3 showed higher ($\bar{x}/\varepsilon$), higher (min/ε) and (max/ε) with higher upper ($U.B./\varepsilon$) and lower bound ($L.B./\varepsilon$) for *C.I.* valued at 252.11%, 166.63%, 388.75%, 237.01% and 267.21%, respectively. In contrast, S1 had the highest *R.I.* and lowest (S/ε) of 9.5 and 17.64%, while S2 had the lowest (R/ε) of 85.71%. S1 displayed the finest statistics for the ratio (tensile/yield) across all of its items, with the exception of the higher ($max/ratio$), which was represented as 112% in S3. Furthermore, S2 had a ratio lower than the standard for all of its specimen. In summary, S2 performed better in yield strength overall, while S1 excelled in tensile strength and ratio. S3 had the highest performance in elongation.

The histograms and PDF curves for the samples from the three specifications are displayed in **Fig. 14.** through **Fig. 23.** These figures represent the outcomes for flexure, arch softening action, catenary action points (ultimate load, displacement, and energy), and total energy. Overall, in this collection of figures, the preceding curve has lower $\bar{x}$, while the flatter one has greater *S* values. Additionally, the majority of the resulting PDF curves exhibited Gaussian characteristics. However, some of the S2 and S3 curves were less smooth due to the small sample size.

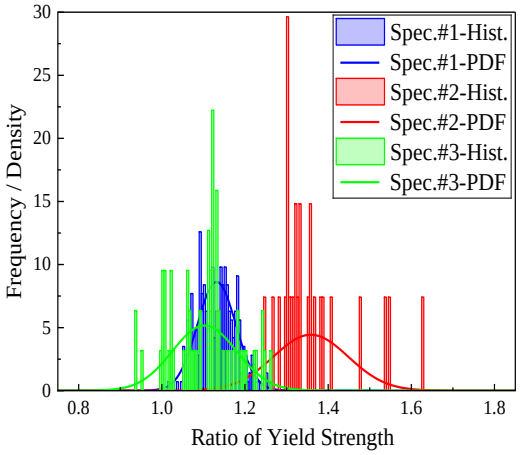

Fig. 10. Histogram and PDF of yield stress for the three specifications' samples

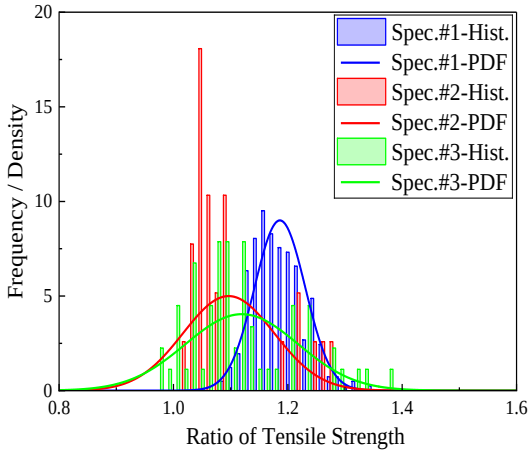

Fig. 11. Histogram and PDF of tensile stress for the three specifications' samples

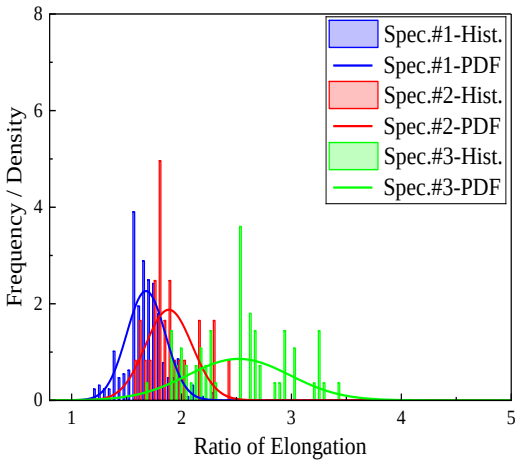

Fig. 12. Histogram and PDF of the elongation for the three specifications' samples

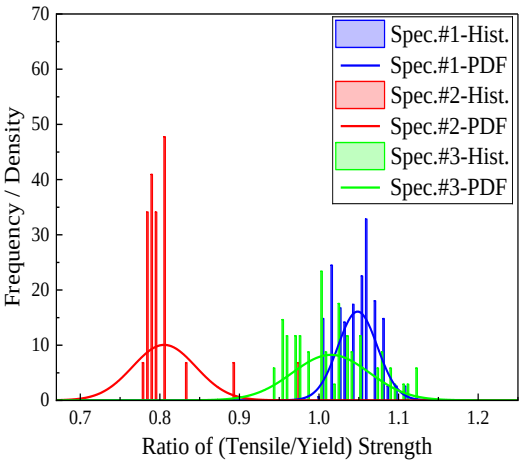

Fig. 13. Histogram and PDF of the ratio (tensile/yield) for the three specifications' samples

Table 5. Key statistics for the collected steel samples as part of BS 4449/05 Gr B500B, ASTM A 615 GR 60 and B500 DWR expressed as ratios of the specification's values.

		Inputs				Outputs									
		Yield	Tensil	Elongati	Ratio	Flexure		Arch		Catenary		Flexure	Arch	Catenary	Total
		F_y	F_u	ε	F_u/F_y	δ_f	P_f	δ_t	P_t	δ_c	P_c	E_f	E_t	E_c	E_{tot}
BS 4449/05 Gr B500B	Spec. Values	500	550	0.05	1.1	179.599	2047.002	601.7639	1348.208	1434.465	2819.818	287625.9786	681576.9853	1679130.187	2648333.151
	$\bar{x}$	113.18	118.63	167.67	104.86	103.91	102.18	99.42	105.05	140.21	143.69	105.36%	101.94%	230.94%	184.10%
	S	4.63%	4.44%	17.64%	2.48%	4.57%	0.64%	0.85%	2.31%	9.54%	8.66%	6.03%	2.25%	33.17%	21.12%
	min.	101.60	109.45	120.00	100.00	100.00	100.30	97.81	99.44	113.03	118.73	100.04%	96.40%	142.25%	127.78%
	max.	126.00	134.36	230.00	110.91	113.87	103.65	99.88	111.32	172.04	182.59	118.61%	106.32%	374.45%	275.64%
	R	24.40	24.91	110.00	10.91	13.87	3.34%	2.07%	11.89	59.01	63.86	18.57%	9.92%	232.20%	147.87%
	R.I.	24.43	26.75	9.5	42.24	22.73	159	116.66	45.51	14.7	16.6	17.47	45.23	6.96	8.72
	99 U.	112.47	117.95	164.97	104.48	103.21	102.08	99.29	104.70	138.74	142.36	104.44%	101.60%	225.86%	180.87%
	C.I L.	113.89	119.31	170.38	105.24	104.62	102.28	99.55	105.41	141.67	145.02	106.29%	102.29%	236.03%	187.34%
ASTM A 615 GR 60	Spec. Values	420	620	0.07	1.476190	167.1129	1989.68	588.3943	1250.497	1782.755	3373.564	260853.1817	657980.0353	2706195.413	3625028.63
	$\bar{x}$	135.83	109.66	188.44	80.56	111.35	105.28	101.75	113.49	140.08	142.69	115.76%	106.06%	221.50%	192.94%
	S	9.01%	7.99%	21.28%	3.97%	5.61%	0.89%	0.83%	4.11%	1.20%	7.23%	7.64%	1.69%	11.10%	8.55%
	min.	124.50	102.19	157.14	77.70	107.48	103.78	100.04	109.01	134.91	135.93	110.40%	101.35%	203.03%	179.10%
	max.	162.90	127.48	242.86	97.30	122.39	107.75	102.15	125.98	140.55	164.97	130.94%	107.88%	254.03%	218.22%
	R	38.40	25.29	85.71%	19.59	14.91	3.96%	2.11%	16.97	5.64%	29.04	20.55%	6.52%	51.00%	39.12%
	R.I.	15.07	13.73	8.86	20.28	19.86	118.20	123.16	27.59	116.87	19.75	15.15	62.93	19.96	22.56
	99 U.	131.01	105.39	177.07	78.43	108.35	104.81	101.31	111.29	139.44	138.83	111.68%	105.16%	215.57%	188.37%
	C.I L.	140.65	113.94	199.82	82.68	114.35	105.76	102.20	115.69	140.72	146.56	119.85%	106.96%	227.44%	197.51%
ES B500 DWR	Spec. Values	500	625	0.08	1.25	179.5992	2047.226	600.9134	1334.893	1957.056	3770.94	287629.2789	683568.2249	3449792.081	4420989.585
	$\bar{x}$	110.26	111.97	252.11	101.51	103.20	101.67	99.68	104.31	127.98	123.96	104.38%	101.06%	170.19%	155.22%
	S	7.73%	9.88%	46.54%	4.84%	5.10%	1.16%	0.84%	4.05%	0.04%	8.60%	6.79%	2.33%	9.61%	7.78%
	min.	93.68	96.80	166.63	94.40	99.98	99.18	97.95	95.92	127.93	109.29	99.79%	96.09%	152.25%	140.37%
	max.	126.40	139.84	388.75	112.00	113.87	103.73	102.06	113.01	128.22	148.09	118.62%	106.03%	194.46%	174.62%
	R	32.72	43.04	222.13	17.60	13.89	4.55%	4.10%	17.09	0.29%	38.80	18.83%	9.95%	42.21%	34.25%
	R.I.	14.26	11.34	5.42	20.96	20.22	87.75	118.83	25.78	3164.0	14.42	15.38	43.44	17.71	19.95
	99 U.	107.67	108.66	236.53	99.89	101.49	101.28	99.40	102.95	127.96	121.08	102.10%	100.28%	166.97%	152.61%
	C.I L.	112.85	115.28	267.69	103.13	104.91	102.06	99.96	105.66	127.99	126.84	106.65%	101.83%	173.41%	157.83%

After analyzing the key statistics and figures for the system response outputs, it can be concluded that S2 had the best performance for flexure (δ_f, P_f), arch action (δ_t, P_t), flexure energy (E_f), arch action energy (E_t), and total energy (E_{tot}). Looking at the flexural performance, the analysis showed that S2 had the highest $\bar{x}/\delta_f$, $\bar{x}/P_f$, min/δ_f, min/P_f, max/δ_f, max/P_f, $U.B./\delta_f$, $U.B./P_f$, $L.B./\delta_f$ and $L.B./P_f$ but achieved the lowest $R.I._{\delta_f}$. However, S1 had the lowest S/δ_f and S/P_f in addition to the highest $R.I._{\delta_f}$ and $R.I_{P_f}$. Additionally, S2 demonstrated better statistics for the arch action performance compared to other systems, although S1 had a slightly lower S/P_t and higher $R.I._{P_t}$ values. In terms of catenary action performance, S1 had the highest $\bar{x}/\delta_c$ and $\bar{x}/P_c$ that slightly outperformed S2. Moreover, it achieved the highest max/δ_c, max/P_c, $U.B./P_c$ and $L.B./\delta_c$ where the last two statistics slightly outperformed S2. On the other hand, S2 slightly outperformed S1 in $U.B./\delta_c$ and $L.B./P_c$. Although S1 and S2 showed competitive catenary action performance, S1 generally showed very low $R.I.$ values coupled with the highest S/δ_c, S/P_c, R/δ_c and R/P_c showing very high dispersion in the catenary action performance. Despite showing the worse catenary action performance, S3 had an outstanding $R.I._{\delta_c}$ value of 3164.09 coupled with a very low S/δ_c value of 0.04% indicating that δ_c is the same for all actual S3 steel. Overall, S2 performed the best in terms of output statistics, except for catenary, where S1 had a slight edge.

For summary, **Fig. 14** to **Fig. 23** visually show the previously shown statistics and its PDF for easier comparison. **Fig. 14.** and **Fig. 15.** present the histogram and PDF for flexural performance metrics. The findings reveal that S2 generally outperformed the other specifications, exhibiting slightly higher $\bar{x}/\delta_f$ and significantly higher $\bar{x}/P_f$. Both S1 and S3 showed similar flexural performance showed in the form of approximately equal $\bar{x}/\delta_f$ and $\bar{x}/P_f$ values.

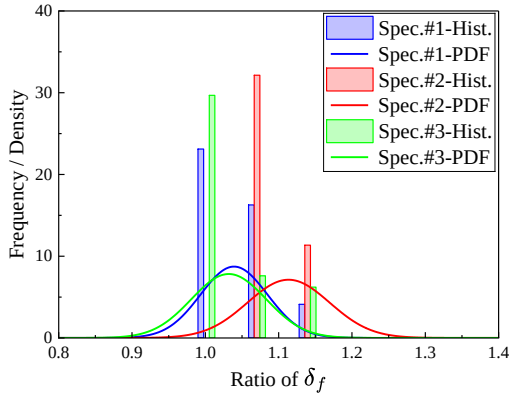

Fig. 14. Histogram and PDF of $\boldsymbol{\delta_f}$ for the three specifications' samples

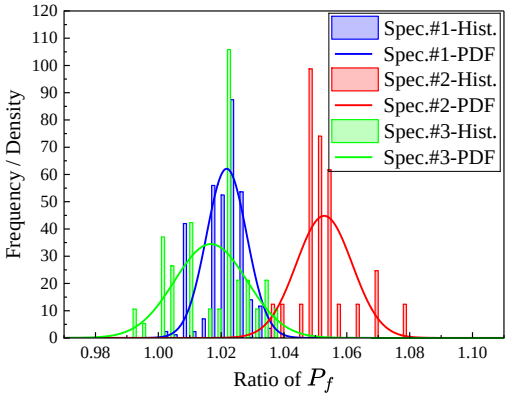

Fig. 15. Histogram and PDF of $\boldsymbol{P_f}$ for the three specifications' samples

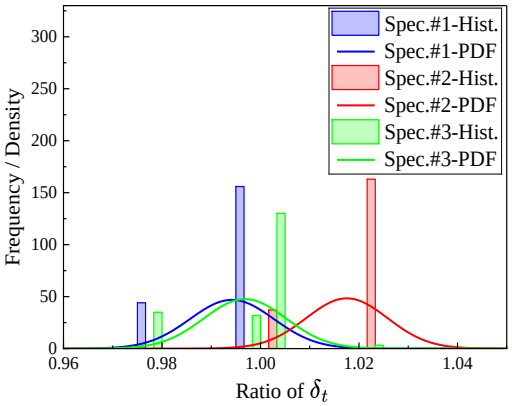

Fig. 16. Histogram and PDF of $\boldsymbol{\delta_t}$ for the three specifications' samples

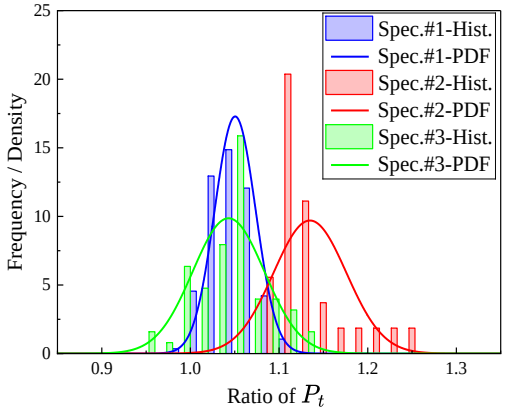

Fig. 17. Histogram and PDF of $\boldsymbol{P_t}$ for the three specifications' samples

Fig. 16. and **Fig. 17.** address the performance metrics related to arch action. Similarly, S2 outpaced the other specifications, showcasing the highest $\bar{x}/\delta_t$ and $\bar{x}/P_t$ while both S1 and S3 showed similar flexural performance showed in the form of approximately equal $\bar{x}/\delta_t$ and $\bar{x}/P_t$ values.

Fig. 18 and **19** concentrate on the metrics for catenary action. The PDFs for S1 and S2 have approximately the same $\bar{x}/\delta_c$ and $\bar{x}/P_c$ values. S1 shows a flat δ_c PDF indicating a wide range of difference between actual and standard values for S1 while S3 shows the opposite behavior where there is a very narrow PDF indicating a narrow difference between actual and standard values.

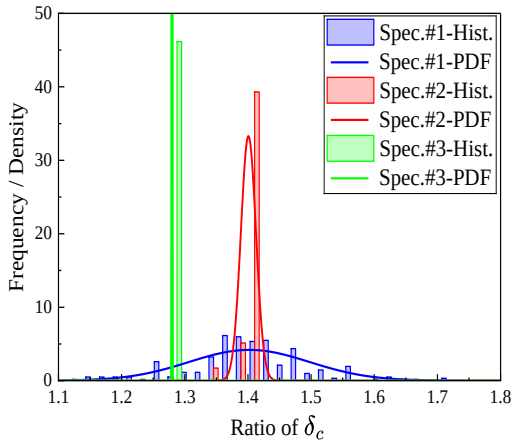

Fig. 18. Histogram and PDF of $\boldsymbol{\delta_c}$ for the three specifications' samples

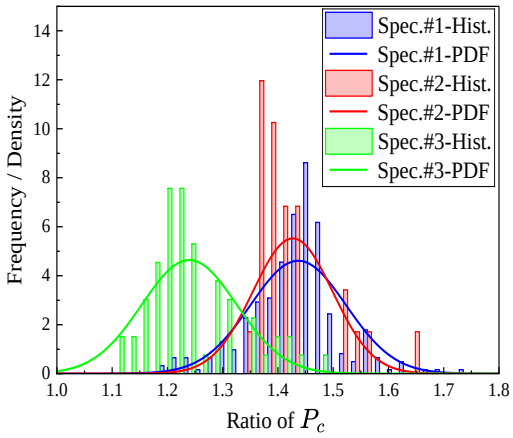

Fig. 19. Histogram and PDF of $\boldsymbol{P_c}$ for the three specifications' samples

Fig. 20 to Fig. 23 display the histograms and PDFs for various energy metrics, such as flexural energy (E_f)arch energy (E_t), catenary energy (E_c), and total energy (E_{tot}). The superiority of S2 in flexural and arch action performance was clearly reflected on higher means for E_f, E_t and E_{tot} while S1 slightly outperforms S2 in E_c.

The **figures**, **14-23**, presented collectively above illustrate the comparative performance of the three specifications in relation to various structural behaviors and energy absorption capacities. The histograms serve as a visual representation of the distribution of each metric, whereas the PDF curves facilitate an understanding of the possibility of various performance results. The analysis indicates that Specification 2 typically demonstrates enhanced performance, making it a preferable choice in construction applications based on the evaluated metrics. This comprehensive examination of the figures helps in understanding the statistical significance and practical implications of the findings outlined in the study.

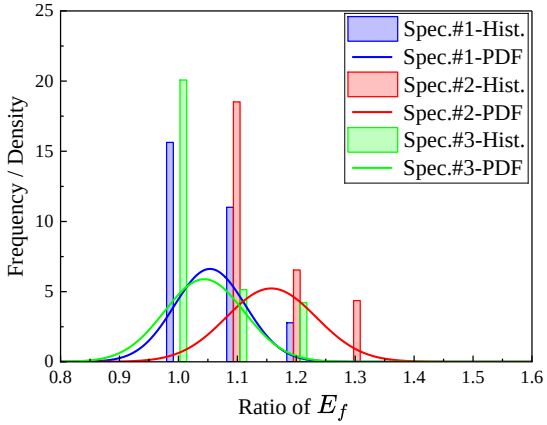

Fig. 20. Histogram and PDF of $\boldsymbol{E_f}$ for the three specifications' samples

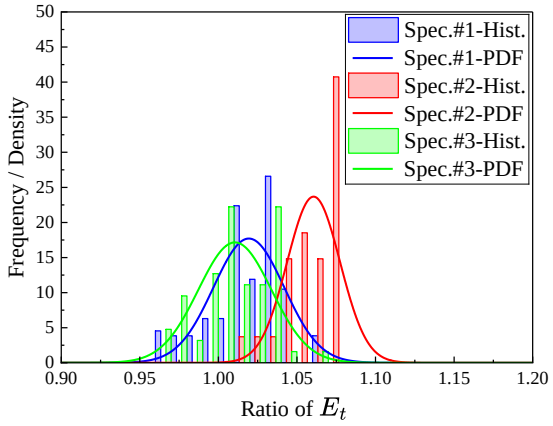

Fig. 21. Histogram and PDF of $\boldsymbol{E_t}$ for the three specifications' samples

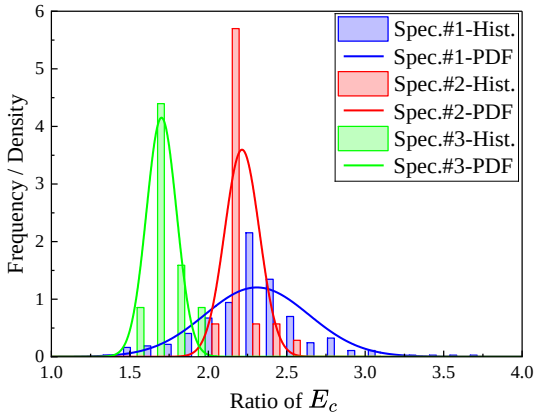

Fig. 22. Histogram and PDF of E_c for the three specifications' samples

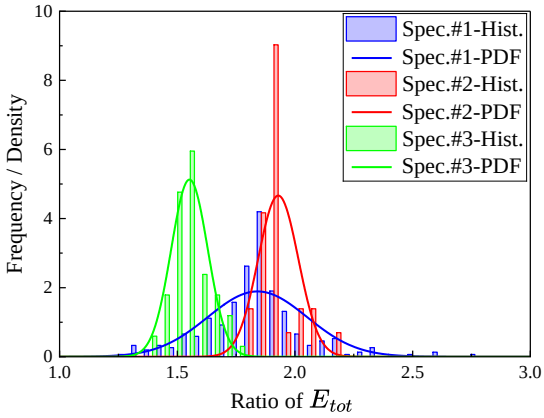

Fig. 23. Histogram and PDF of E_{tot} for the three specifications' samples

To evaluate the relation between inputs and outputs, the correlation coefficients $\rho(x, y)$, displayed in **Table 6.**, were assessed to examine the correlation between various inputs and outputs, **Table 7.** describes the correlation coefficient values. The yield stress of the three specifications exhibited almost perfect correlation with P_t and very strong correlation with P_f. This very strong correlation happened also for S2 and S3 for δ_f, P_c, E_f, E_c, and E_{tot} and; likewise, the yield strength demonstrated moderate and strong correlation with δ_c for S2 and S3, respectively. In contrast, the other correlations for S1 ranged from very weak for δ_c to strong for the rest of outputs. Additionally, the three specifications displayed negative strong correlation with δ_t, while E_t showed negative moderate, negative strong and negative very weak with S1, S2 and S3 respectively. Furthermore, even with smaller correlation value, the tensile strength generally exhibited the same behavior as yield stress in terms of positive and negative correlations with outputs. The highest and lowest positive correlations were found between yield strength and P_t and between yield strength and δ_c in S2 and S1, at 0.999 and 0.052, respectively. In S2, δ_t had the highest negative correlation with a value of -0.878 with tensile strength, while in S3, E_t had the lowest negative correlation with a value of -0.090 with yield strength.

Table 6. Correlation relations between inputs and outputs

		Flexure		Arch		Catenary		Flexure	Arch	Catenary	Total
		δ_f	P_f	δ_t	P_t	δ_c	P_c	E_f	E_t	E_c	E_{tot}
S1	Yield	0.640	0.949	-0.666	0.987	0.052	0.481	0.647	-0.355	0.226	0.235
	Tensile	0.536	0.767	-0.747	0.850	0.117	0.564	0.542	-0.388	0.292	0.297
	Elongation	0.024	0.062	0.156	-0.007	0.994	0.869	0.024	0.060	0.975	0.973
	Ratio	-0.254	-0.424	-0.031	-0.358	0.105	0.070	-0.257	-0.001	0.081	0.073
S2	Yield	0.881	0.985	-0.862	0.999	0.115	0.939	0.885	-0.593	0.929	0.935
	Tensile	0.672	0.707	-0.878	0.796	0.184	0.927	0.674	-0.563	0.856	0.852
	Elongation	0.308	0.249	-0.593	0.314	0.470	0.473	0.308	-0.453	0.501	0.489
	Ratio	-0.175	-0.275	-0.150	-0.153	0.133	0.134	-0.176	-0.056	0.039	0.024
S3	Yield	0.758	0.986	-0.707	0.998	0.563	0.929	0.768	-0.090	0.969	0.973
	Tensile	0.724	0.795	-0.781	0.864	0.416	0.946	0.730	-0.261	0.924	0.920
	Elongation	-0.226	-0.134	0.368	-0.246	0.180	-0.429	-0.227	0.189	-0.355	-0.347
	Ratio	0.185	-0.021	-0.354	0.083	-0.073	0.333	0.182	-0.334	0.234	0.220

In contrast to yielding and tensile strengths, the elongation displayed a different pattern of correlations. S1 had a nearly perfect positive correlation with δ_c, a very strong positive correlation with P_c, E_c and E_{tot}, and a very weak positive correlation with other outputs, except P_t, which showed a very weak negative correlation. In addition, S2 had a positive moderate correlation with all outputs except δ_t, E_t which had strong and moderate negative correlations. S3 had moderate positive

correlation with δ_t, very weak positive correlation with δ_c and E_t, very weak negative correlation with δ_f, P_f, P_t and E_f and moderate negative correlation with the remaining outputs. In terms of the ratio (tensile/yield) stress, both S1 and S2 demonstrated very weak positive correlation with δ_c , P_c, ,E_c and E_{tot} and very weak to moderate negative correlations with flexure (δ_f, P_f), arch action (δ_t, P_t), E_f and E_t. With a slightly different behavior, S3 exhibited very weak positive correlations with both δ_f, P_t, E_f, E_c and E_{tot} with moderate correlation P_c, while it showed also a very weak negative correlations with P_f and δ_c and moderate negative correlation with δ_t and E_t. Generally, **Table 6** reveals that the correlation coefficient between δ_c and other mechanical properties ranges from 0.052 to 0.563, except for elongation in S1 and the ratio in S3. This range indicates a weak to strong relationship, as detailed in **Table 7**. Consequently, δ_c cannot be reliably predicted based solely on the mechanical properties of the samples. The aforementioned claim with facts mentioned in the beginning of section 4 explains why the final displacement for most specimens in **Fig. 9.** were very close despite the differences in the mechanical properties.

Table 7. Description of correlation values

Correlation Coefficient Value	Description
$0 \leq \ \rho(x,y) \ < 0.25$	very weak
$0.25 \leq \ \rho(x,y) \ < 0.50$	moderate
$0.50 \leq \ \rho(x,y) \ < 0.75$	strong
$0.75 \leq \ \rho(x,y) \ < 0.99$	very strong
$0.99 \leq \ \rho(x,y) \ \leq 1$	perfect

The analysis indicates that Specification 2 (S2) outperforms the others Specifications across multiple metrics, suggesting it may be the most suitable choice for construction applications where structural integrity and resilience are paramount. The superior performance of S2 in energy absorption and load-bearing capacity implies that structures designed with this specification may have enhanced safety margins, particularly in scenarios involving progressive collapse. The findings of this study also highlight a potential gap between current design standards and the actual performance of available materials raising a concern that existing standards may underestimate the capabilities of modern reinforcement steels, which could lead to over-engineering or unnecessary material use.

5.3 Test of Hypothesis

This study highlights two significant queries regarding the data collected. The first query examines whether each of the three specifications statistically meets the standard requirements for usage in construction process. The second query is to determine if there is notable variance among the specifications that would justify choosing one over the others based on extra benefits, such as abundance or cost-effectiveness, instead of just standard values. The hypothesis test about single mean provides an answer to the first query. This was undertaken when determining the confidence interval (CI) for each specification, where its lower bound exceeded the necessary standard's value in every case. Testing the alternative hypothesis, $H_1 : |\mu_1 - \mu_2| > 0$, against the null hypothesis, $H_o : \mu_1 - \mu_2 = 0$, provides the answer to the second query. The null hypothesis for one sided critical region is accepted, if the critical region, $t' < t_{\alpha,\nu}$. This is done under the assumption that the two populations' variance are unknowns and unequal also which is called Behrens-Fisher problem [50], where, and as shown in **Eq. (4)**

$$t' = \left|\bar{x}_1 - \bar{x}_2\right| / \sqrt{\frac{S_1^2}{n_1} + \frac{S_2^2}{n_2}} \tag{4}$$

providing ν is the approximate degree of freedom, called Satterthwaite's approximation, given as shown in **Eq. (5)**:

$$\nu = \left(\frac{S_1^2}{n_1} + \frac{S_2^2}{n_2} \right)^2 \Bigg/ \left(\frac{\left(\frac{S_1^2}{n_1} \right)^2}{n_1 - 1} + \frac{\left(\frac{S_2^2}{n_2} \right)^2}{n_2 - 1} \right) \quad (5)$$

Table 8. Decision about H_o

		f_y	f_u	ε	f_y/f_u
S1 and S2	t'	12.9	5.75	4.92	31.23
	tα/2,v	2.47	2.47	2.46	2.47
	P-value	2.33e-13	1.80e-06	1.60e-05	0
	Decision	Rejected	Rejected	Rejected	Rejected
S1 and S3	t'	2.89	5.24	14.18	5.34
	tα/2,v	2.38	2.38	2.38	2.38
	P-value	0.00256	8.70e-07	0	5.60e-07
	Decision	Rejected	Rejected	Rejected	Rejected
S2 and S3	t'	12.86	1.17	8.9	21.42
	tα/2,v	2.42	2.39	2.37	2.39
	P-value	1.11e-16	0.12416	3.26e-14	0
	Decision	Rejected	Accepted	Rejected	Rejected

The tests and p-value of sample data for each specification with others at $\alpha = 1\%$, are then calculated using **Eq. (4)** and **(5)**, where the results are tabulated in Table 8. These results demonstrated that S2 and S3 could be used interchangeably for tensile stress only. Otherwise, there are significant differences in mean values between any two specifications for all inputs, favoring the specification with the higher mean.

The above discussion provides few key insights that could advance the current state of knowledge in this field as presented below:

1. Mechanical properties of reinforcement steel frequently used in construction often exceed the minimum requirements set by current standards. This finding shows that current design practices may underestimate the accurate capacity and resilience of structures.
2. Due to this difference, current design standards may not truly represent the full potential of reinforcement steel. Current design codes may underestimate the progressive collapse resistance of structures. This could explain why some buildings do not collapse when a major load carrying member collapses as shown in Fig. 1. in the manuscript. This insight emphasizes the need to consider the actual properties of steel in the design practices rather than relying solely on standardized values, which may not reflect real-world conditions.
3. The study findings advocate for a revision of current design codes to better align with the actual performance of reinforcement steel. This could lead to improved safety and reliability of structures.
4. By investigating the relationship between reinforcement steel properties and structural performance, the study enhances the knowledge of the mechanisms that result in progressive structural collapse. This knowledge is crucial for developing more effective design practices and mitigation measures to enhance the resilience of structures.
5. The use of statistical tools to measure differences in material properties and establish predictive correlations for structural behavior represents an advancement in the methodology of structural analysis. This approach can lead to more informed decision-making and better risk assessment in engineering practice.

6 Conclusions

This study focused on numerically and analytically investigating the reliability of using reinforcement steel in compliance with current ASTM A615/A615M, BS 4449:2005, and ES 262-

2/2015 standards in RC framed structures to resist disproportionate structural collapse. The study employed 2D fiber element (FE) models to replicate how structures respond to progressive collapse caused by the loss of columns.

The study revealed that the steel used frequently in RC framed structures often surpasses the minimum requirements set by the standards in terms of mechanical properties. The difference in performance between the steel used and the set standards resulted in an inaccurate assessment of the structure capacity and resilience to resist progressive collapse in design processes.

This finding is significant because it implies that the current design standards may not truly represent the full potential of reinforcement steel. It highlights the significance of accurately assessing the mechanical properties of the steel so that engineers can better assess the behavior and sustainability of structures. The research also underscores the need to update and revise current design standards to better match the real performance of construction materials.

The significance of the study is its indication that current design standards may not truly represent the full potential of construction material properties, specifically reinforcement steel, and can compromise safety, reliability, and longevity of the structures against progressive collapse. The study shows that reinforcement steel frequently used in structures has higher mechanical properties than the standard material minimum permissible properties used in the design process and can; therefore, result in more sustainable structures.

Addressing the significance of this study in existing standards can be twofold, 1) material property data from literature and manufacturers can be collected and used to update and revise existing design standards to reflect the actual performance of construction materials, specifically reinforcement steel; this may require collaboration with regulatory entities and professional organizations to apply the revisions, 2) ensure that engineers are mindful of the applied revisions and know how to apply them in their design.

However, three distinct steel grades were the subject of this investigation, which limit the generalization of results. Additional research should investigate more different steel grades with a large sample size with adequately diverse data.

In conclusion, the study underlines the need for a thorough understanding of the material mechanical properties, particularly reinforcement steel, and importance of incorporating this knowledge into design standards to improve the reliability and longevity of RC buildings when subjected to progressive collapse as a result of column exclusion.

Funding Statement

This work was supported by Research Office, Emirates Center for Mobility Research at the United Arab Emirates University [fund number 12R150].

CRediT authorship contribution statement

Omer: Software, Data curation, Validation, Investigation, Formal analysis, Writing- Original draft preparation. **Said**: Conceptualization, Methodology, Investigation, Formal analysis, Supervision, Software, Data curation, Validation. **Osama**: Methodology, Software, Data curation, Validation, Investigation, Formal analysis, Writing- Original draft preparation. **Bilal**: Funding acquisition, Administration, Supervision, Methodology, Writing- Original draft preparation, Writing- Reviewing and Editing.

Conflicts of Interest

The authors declare that they have no conflicts of interest to report regarding the present study.

Data Availability Statement

Some or all data, models, or codes that support the findings of this study are available from the corresponding author upon reasonable request.

References

[1] US General Service Administration (GSA). Progressive Collapse Analysis and Design Guidelines for New Federal Office Buildings and Major Modernization Projects. 2003.

[2] Yi WJ, Yi F, Zhou Y. Experimental studies on progressive collapse behavior of RC frame structures: advances and future needs. International Journal of Concrete Structures and Materials 2021; 15(1): 000469. https:// doi.org/10.1186/s40069-021-00469-6.

[3] Li S, Shan S, Zhai C, Xie L. Experimental and numerical study on progressive collapse process of RC frames with full-height infill walls. Engineering Failure Analysis 2016; 59: 57-68. https://doi.org/10. 1016/j.engfail anal.2015.11.020.

[4] de Normalisation, C. C. E. (2006). EN 1991-1-7: Eurocode 1–Actions on Structures–Part 1–7: General Actions–Accidental Actions. Brussels (Belgium): CEN.

[5] ASCE/SEI. Minimum design loads and associated criteria for buildings and other structures. American Society of Civil Engineers (ASCE), 2017. https://doi.org/10.1061/9780784414248.

[6] British Standards Institution (BSI). BS 8110: Structural Use of Concrete – Code of Practice for Design and Construction. 1997. https://doi.org/10.3403/BS8110.

[7] US Department of Defense (DoD). Unified Facility Criteria (UFC) Design of buildings to resist progressive collapse. 2016

[8] Fascetti A, Kunnath SK, Nisticò N. Robustness evaluation of RC frame buildings to progressive collapse. Engineering Structures 2015; 86: 242-249. https://doi.org/10.1016/j.engstruct.2015.01.008.

[9] Ibrahim AR, Makhloof DA, Ren X. Probabilistic progressive collapse assessment for RC framed-wall structure. Structures 2023; 48: 551-575. https://doi.org/10.1016/j.istruc.2022.12.115.

[10] Elkady N, Augusthus Nelson L, Weekes L, Makoond N, Buitrago M. Progressive collapse: Past, present, future and beyond. Structures 2024; 62: 106131. https://doi.org/10.1016/j.istruc.2024.106131.

[11] El-Ariss, B., Elkholy, S. and Shehada, A., United Arab Emirates University, 2024. Internal reinforcement method of upgrading progressive collapse resistance of reinforced concrete framed system. U.S. Patent 12,116,791.

[12] Weng J, Lee CK, Tan KH, Lim NS. Damage assessment for reinforced concrete frames subject to progressive collapse. Engineering Structures 2017; 149: 147-160. https://doi.org/10.1016/j.engstruct.2016.07.038.

[13] Abedini M, Mutalib AA. Investigation into damage criterion and failure modes of RC structures when subjected to extreme dynamic loads. Archives of Computational Methods in Engineering 2020; 27(2): 501-515. https://doi.org/10.1007/s11831-019-09317-z.

[14] Sangiorgio V, Uva G, Fatiguso F, Adam JM. A new index to evaluate exposure and potential damage to RC building structures in coastal areas. Engineering Failure Analysis 2019; 100: 439-455. https://doi.org/10.101 6/j.engfailanal.2019.02.052.

[15] Abedini M, Zhang C. Dynamic performance of concrete columns retrofitted with FRP using segment pressure technique. Composites Structures 2021; 260: 113473. https://doi.org/10.1016/j. compstruct.2020. 1 13473.

[16] Scalvenzi M, Gargiulo S, Freddi F, Parisi F. Impact of seismic retrofitting on progressive collapse resistance of RC frame structures. Engineering Failure Analysis 2022; 131: 105840. https://doi.org/10.1016/j.engfailan al.2021.105840.

[17] Kumar P, Lavendra S, Raghavendra T. Progressive collapse resistance of reinforced concrete frame structures subjected to column removal scenario. Materials Today: Proceedings 2022; 61: 264-274. https://doi.o rg/10. 1016/j.matpr.2021.09.204.

[18] Ellingwood B, Galambos TV. Probability-based criteria for structural design. Structural Safety 1982; 1(1): 15-26. https://doi.org/10.1016/0167-4730(82)90012-1.

[19] Le JL, Xue B. Probabilistic analysis of reinforced concrete frame structures against progressive collapse. Engineering Structures 2014; 76: 313-323. https://doi.org/10.1016/j.engstruct.2014.07.016.

[20] Li Y, Lu X, Guan H, Ren P, Qian L. Probability-based progressive collapse-resistant assessment for reinforced concrete frame structures. Advances in Structural Engineering 2016; 19(11): 1723-1735. https:// doi.org/10.1177/1369433216649385.

[21] Zhang Q, Zhao YG, Kolozvari K, Xu L. Reliability analysis of reinforced concrete structure against progressive collapse. Reliability Engineering & System Safety 2022; 228: 108831. https://doi.org/0.1016/1j. ress.2022.108831.

[22] Xue B, Le JL. Stochastic computational model for progressive collapse of reinforced concrete buildings. Journal of Structural Engineering. 2016;142(7):04016031. https://doi.org/10.1061/(ASCE)ST.1943-541X.0001485.

[23] Xie SC, Feng DC. Reliability assessment of reinforced concrete structures subjected to progressive collapse. 2019. https://doi.org/10.22725/ICASP13.063.

[24] Zhou Y, Zhang B, Luo X, Hwang HJ, Zheng P, Zhu Z, Yi W, Kang SM. Reliability of fully assembled precast

concrete frame structures against progressive collapse. Journal of Building Engineering 2022; 51: 104362. https://doi.org/10.1016/j.jobe.2022.104362.
[25] Ding Y, Song X, Zhu HT. Probabilistic progressive collapse analysis of steel-concrete composite floor systems. Journal of Constructional Steel Research 2017; 129: 129-140. https://doi.org/10.1016/j.j csr.2016.11.009.
[26] Vazna RV, Zarrin M. Sensitivity analysis of double layer Diamatic dome space structure collapse behavior. Engineering Structures 2020; 212: 110511. https://doi.org/10.1016/j.engstruct.2020.110511.
[27] Ibrahim AR, Makhloof DA, Ren X. Probabilistic progressive collapse assessment for RC framed-wall structure. Structures 2023; 48: 551-575. https://doi.org/10.1016/j.istruc.2022.12.115.
[28] Shaijal KM, Pandikkadavath MS, Mangalathu S, Davis R. Material uncertainty based seismic robustness assessment of steel moment-resisting frames. In: Proceedings of the 12th International Conference on Advances in Steel Structures. 2022; 485–494. https://doi.org/10.1007/978-981-16-7397-9_35.
[29] Qian K, Li JS, Huang T, Weng YH, Deng XF. Punching shear strength of corroded reinforced concrete slab-column connections. Journal of Building Engineering 2022; 45: 103489. https://doi.org/10.1016/j.jobe.2021.103489.
[30] Zhang X, Zhao Y, Zhu Z, Sha S, Lv C. Experimental study on the cyclic bond behavior of corroded rebar based on modified beam test. Journal of Building Engineering 2022; 47: 103834. https://doi.org/10.1016/j.jobe.2021.103834.
[31] Yu XH, Qian K, Lu DG, Li B. Progressive collapse behavior of aging reinforced concrete structures considering corrosion effects. Journal of Performance of Constructed Facilities 2017; 31(4): 04017009. https://doi.org/10.1061/(ASCE)CF.1943-5509.0001001.
[32] Qin JG, Zhang WW, Huang T, Qian K, Deng XF. Effect of steel reinforcement corrosion on progressive collapse resistance of beam-slab structure with interior column failure. Engineering Structures 2024; 312: 118257. https://doi.org/10.1016/j.engstruct.2024.118257.
[33] Feng DC, Xie SC, Li Y, Jin L. Time-dependent reliability-based redundancy assessment of deteriorated RC structures against progressive collapse considering corrosion effect. Structural Safety 2021; 89: 102061. https://doi.org/10.1016/j.strusafe.2020.102061.
[34] Elsayed WM, Abdel Moaty MAN, Issa ME. Effect of reinforcing steel debonding on RC frame performance in resisting progressive collapse. HBRC Journal 2016; 12(3): 242–254. https://doi.org/10.1016/j.hbrcj.2015.02.005.
[35] Jagatheswari P, Ramasubramani R. Nonlinear static analysis study on progressive collapse behaviour of 2D RC frame with different grades of steel. In: Proceedings of the conference on structural and civil engineering; 2024. p. 201–215. https://doi.org/10.1007/978-981-99-6175-7_20.
[36] Alrubaidi M, Alhammadi SA. Numerical investigation on progressive collapse mitigation of steel beam–column joint using steel plates. Materials. 2022;15(21):7628. https://doi.org/10.3390/ma15217628.
[37] ASTM. Designation: A615/A615M-12 American Association State Highway and Transportation Officials Standard Specification for Deformed and Plain Carbon-Steel Bars for Concrete Reinforcement. 2012. https://doi.org/10.1520/A0615_A0615M-12.
[38] British Standards Institution (BSI). BS 4449: Steel for the Reinforcement of Concrete – Weldable Reinforcing Steel – Bar, Coil and Decoiled Product – Specification. 2005. https://doi.org/10.3403/30109892U.
[39] Egyptian Organization for Standards & Quality (ES). ES:262-2 /2015 ISO: 6935-2/2007 Steel for the Reinforcement of Concrete Part 2 Ribbed bars Arab Republic of Egypt. https://www.eos.org.eg/en/standard/15250. 2021 (Accessed 13 June 2024)
[40] Makoond, N., Shahnazi, G., Buitrago, M., & Adam, J. M. (2023). Corner-column failure scenarios in building structures: Current knowledge and future prospects. Structures, 49, 958–982. https://doi.org/10.1016/j.istruc.2023.01.121
[41] American Society of Testing and Materials (ASTM). Steel Standards. https://www.astm.org/products-services/standards-and-publications/standards/steel-standards.html#section2, (accessed 13 June 2024)
[42] Seismosoft INC. SeismoStruct 2023 - A Computer Program for Static and Dynamic Nonlinear Analysis of Framed structures. 2023. https://seismosoft.com/product/seismostruct/ (accessed 13 June 2024)
[43] El-Ariss B, Elkholy S, Shehada A. Benchmark numerical model for progressive collapse analysis of RC beam-column sub-assemblages. Buildings 2022; 12(2): 122. https://doi.org/10.3390/buildings12020122.
[44] Elkholy S, Shehada A, El-Ariss B. Innovative scheme for RC building progressive collapse prevention. Engineering Failure Analysis 2023; 154: 107638. https://doi.org/10.1016/j.engfailanal.2023.107638.
[45] Elkholy S, Shehada A, El-Ariss B. Effects of floor system on progressive collapse behavior of RC frame sub-assemblages. Buildings 2022; 12(6): 737. https://doi.org/10.3390/buildings12060737.
[46] Shehada A, Elkholy S, El-Ariss B. Numerical progressive collapse analysis of RC framed structures. Proceedings of the 6th World Congress on Civil, Structural, and Environmental Engineering (CSEE'21) 2021. https://doi.org/10.11159/icsect21.lx.105.

[47] El-Ariss B, Elkholy SA. Scheme for beam progressive collapse mitigation. International Journal of Structural Engineering 2018; 9(3): 175. https://doi.org/10.1504/IJSTRUCTE.2018.093672.
[48] Elkholy S, El-Ariss B. Enhanced external progressive collapse mitigation scheme for RC structures. International Journal of Structural Engineering 2016; 7(1): 63. https://doi.org/10.1504/IJSTRU CTE.2016.0 73679.
[49] The Math Works, "The Math Works, Inc. MATLAB. Version 2020a, Computer software.," 2020.
[50] Walpole R, Myres R, Myres S, Ye K. Probability Statistics for Engineers and Scientists; 9th edition 2011
[51] Nowak AS, Collins KR. Reliability of Structures. CRC Press 2012. https://doi.org/10.1201/b12913.